Estimation of the background to W+jets and Z+jets.

Geoff Manning

January 20, 1995

Fermi National Accelerator Laboratory Batavia, Illinois, 60510

1 Introduction

$W \to e\nu$ +jets can have background from jets that fake the electron signature, or from genuine electrons that come from a source other than $W \to e\nu$. The standard method to estimate the background is to use the spectra for bad electrons to correct the spectra for good electrons. The normalization is determined by comparing the missing transverse energy plots for low missing transverse energy, typically for less than 18 GeV. This procedure makes no attempt to identify the origin of the background. This paper gives an alternative procedure that unfolds spectra into components from electrons and from fake electrons. It provides as output estimates of the corrected signal from electrons and that from the fake electrons. Results from the two procedures are compared. The fitting procedure is then applied to Z+jets using the parameters determined from the W+jets analysis.

2 Definition of good and bad electron

All events for this analysis are from run 1a and are taken with the Electron_High trigger. The trigger requirements are:

- electron transverse energy > 20 GeV
- isolation < 0.4 (or 0.6 for part of the run)

2.1 Selection of good electrons

All electrons in the sample of potential $W \to e\nu$ +jets events satisfy the following criteria:

- fraction EM > 0.9
- number of cells at least 20
- it was the most energetic electron candidate satisfying the above cuts
- transverse energy > 25 GeV

Good electrons in addition satisfy the following cuts:

- $\chi^2 < 100$
- $\sigma_{track} < 5$
- Iso < 0.1

Where:

- χ^2 is the H-matrix χ^2
- $\sigma_{track} = \sqrt{(\frac{r\Delta\phi}{r\delta\phi})^2 + (\frac{\Delta z}{\delta z})^2}$
- Iso $= \frac{E^{total}_{\Delta r=0.4} - E^{EM}_{\Delta r=0.2}}{E^{EM}_{\Delta r=0.2}}$

2.2 Selection of bad electrons

A scoring system is defined to measure the degree to which any electron fails to make the "good" qualification. Table 1 defines scores for electrons failing to meet the requirements for good for each of the three tests above. A total quality score for an electron is the sum of the scores for each test. A score of zero defines a good electron and a score above zero is a bad electron with higher scores indicating an increasingly poorer fit. For the standard method a cut of > 12.4 is used to define a class of very bad electrons. The choice of 12.4 is a compromise between a very stringent criteria for very bad and a need to have a reasonable population for statistical accuracy. For the fitting procedure an electron with any score above zero is defined as bad.

For electron 2 a quality score of 100 is added if the EM fraction is less than 0.9 and a further 200 is added if the number of cells is less than 20.

Table 1: Quality scores for electrons. Total score is the sum of scores for χ^2, σ_{track}, and ISO.

	value	score	value	score	value	score
χ^2	< 100	0	$100 < \chi^2 < 250$	1.2	> 250	10.6
σ_{track}	< 5	0	$5 < \sigma_{track} < 10$	1.1	> 10	10.3
ISO	< 0.1	0	$0.1 < ISO < 0.2$	1.0	> 0.2	10.0

3 Standard Method

3.1 Procedure for background subtraction

The spectra of missing transverse energy, $\not{E}_T$, for good and bad electrons are compared and a normalization constant, α, determined so that the areas are equal below 18 GeV. Figure 1 shows the spectra for all W events, for:

- good electrons, $\not{E}_T$ (G)
- for bad electrons, $\not{E}_T$ (B), and for
- $\not{E}_T$ $(Signal) = \not{E}_T$ $(S) = \not{E}_T$ $(G) - \alpha$ $\not{E}_T$ (B).

The subtracted spectrum shows that the fit below 18 GeV is not perfect - there is an energy shift to higher energies of about 0.3 GeV for the bad electron spectrum. Nevertheless a clean W signal remains above 20 GeV. The same normalization constant is used for treatment of the transverse mass,$M_T^{e\nu}$, for events with $\not{E}_T$ $> 25 GeV$. A very clean signal is seen at the W mass, see Fig. 2. Events between 50 and 95 GeV/c^2 in the subtracted spectrum are taken as the W signal. The errors shown are statistical with no allowance for systematic errors.

3.2 Criteria for jets.

Jets are formed with the standard procedure with a cone size of 0.5, a lower energy cut of 15 GeV, and $\mid \eta \mid < 2.5$. Jets that align with a good electron are excluded since the jet list initially includes all electrons. Only one and two electron candidates are included in the Ntuple and hence, for completeness, a very small correction is required to allow for events with three or more good electrons. This very small correction has not been made in this analysis. Jets that align with a good electron with dr $<$ 0.2 are excluded from the jet list, where
$dr = \sqrt{(\eta_e - \eta_{jet})^2 + (\phi_e - \phi_{jet})^2}$
For bad electrons the jet list still includes the bad electron, or jet faking the electron. For events with a second good electron, e.g. $Z \rightarrow e^+e^-$ events, any jet aligning with either good electron is excluded from the jet list. $W \rightarrow e\nu$ events can be accompanied with 0, 1, 2, —-N jets. Good electron events can be separated into subgroups by the number of jets in the event. No double counting is involved since jets aligned with good electrons are removed from the jet list. For the corresponding bad electron sample allowance has to be made for the fact that the bad electrons will also be included in the jet list. For $W \rightarrow e\nu$ events one jet has to be subtracted from the jet list for the bad electron events.

3.3 Results for $W \to e\nu$ +jets using standard method

Figure 3 shows the plots of $M_T^{e\nu}$(S)($\not\!\!E_T$> 25) for W+0jets, W+1jet, W+2jets and W+3jets. A clear signal is seen for W+0jets and W+1jet; but the signal for W+3jets is much less clear. Table 2 provides the results for the inclusive channel W+all, and for the exclusive channels; W+0jets, W+1jet, W+2jets, and W+3jets. Table 2 includes, for each channel:

- N(G), the number of good electron events with $\not\!\!E_T$ $> 25GeV$ and $50 <$ $M_T^{e\nu}$ $< 95GeV/c^2$
- α, the normalization constant for the background subtraction
- $\alpha N(B)$, the number of background events subtracted with $\not\!\!E_T$ $> 25GeV$ and $50 <$ $M_T^{e\nu}$ $< 95GeV/c^2$
- $N(S) = N(G) - \alpha N(B)$, the resulting signal
- and the percentage background $= \frac{\alpha N(B)}{N(G)-\alpha N(B)}$

Table 2: Results for standard method.

	N(G)	α	αN(B)	N(S)	%Background
W+all	9673 ± 98	1.021	245 ± 16	9428 ± 100	2.6%
W+0jets	8291 ± 90	1.298	171 ± 15	8120 ± 92	2.1%
W+1jet	1146 ± 34	0.997	73 ± 9	1073 ± 35	6.8%
W+2jets	196 ± 14	0.901	22 ± 4.4	174 ± 15	12%
W+3jets	32 ± 5.7	0.885	6.2 ± 2.3	25.8 ± 6.1	24%

3.4 Problems with the standard procedure

The procedure to subtract the background is empirical and a number of uncertainties and shortcomings exist.These include:

- The procedure provides no understanding of the origin of the background. There can be contributions to the good electron spectrum that come from fake electrons, and from real electrons that are not from $W \to e\nu$. The bad electron sample can include real electrons that are in the tail of the distributions of the three variables used to classify the electrons, as well as fake electrons. No estimate of these different contributions is made in the background subtraction process.
- The $\not\!\!E_T$ spectra for good and bad electrons do not fit perfectly below 18 GeV - the bad electron electron peaks at about 0.3 GeV higher energy than the good electron spectrum. The subtracted $\not\!\!E_T$ spectra, $\not\!\!E_T$(S), for W+all is shown in Fig. 1 and for W+0jets, W+1jet, W+2jets, and W+3jets in Fig. 4.

- The normalization below 18 GeV of the spectra has to be determined for each channel (see Table 2).
- The background subtracted in the plots for events with $\not{E}_T > 25GeV$, peak at the W mass - see Fig. 5. This could be because with a definition for a bad electron being a score > 12.4 the spectrum for bad electrons still includes some good electrons, or because the fake background itself peaks at the W mass. The procedure gives no way of investigating the background.
- The procedure gives no estimate of real electrons coming from a channel other than $W \rightarrow e\nu$ and whether these contribute to the signal derived for $W \rightarrow e\nu$.

Nevertheless the procedure works providing the definition for bad electrons is made very hard. A requirement that at least $\chi^2 > 200$ and $\sigma_{track} > 10$ keeps the good electron tail in the bad electron sample very small. The fraction subtracted from the good electron spectra of $M_T^{e\nu}$ with $\not{E}_T > 25GeV$ is small and the shortcomings listed above do not play a major part.

Despite this there is advantage in developing an alternative procedure that overcomes some of the shortcomings listed.

4 Fitting Method

4.1 Procedure used

The aim of the fitting procedure is to unfold any plotted spectrum into two components, that from real electrons including sources other than $W \rightarrow e\nu$ and that from fakes that masquerade as electrons. The main contribution to fakes is QCD produced jets where one jet has a large EM fraction and it satisfies the trigger requirements. Some fraction, ε_{GF}, of these events will satisfy the constraints for a good electron. The rest of the fake events will be classified as bad electrons with an efficiency ε_{BF}. Since for this method all electrons are good or bad (bad is taken to be any score greater than zero), $\varepsilon_{GF} + \varepsilon_{BF} = 1$. For a perfect detector ε_{GF} would be zero.

Genuine electrons have an efficiency,ε_{GE}, of satisfying the cuts for a good electron and $(1 - \varepsilon_{GE})$ as the efficiency for failing the cuts.

Any spectrum , V, of some variable can be produced for good electrons, V(G), and for bad electrons, V(B). These spectra can be unfolded into components of the spectrum for real electrons, V(E), and that for fakes, V(F).

$$V(G) = \varepsilon_{GE} V(E) + (1 - \varepsilon_{BF}) V(F) \quad (1)$$
$$V(B) = (1 - \varepsilon_{GE}) V(E) + \varepsilon_{BF} V(F) \quad (2)$$

The above expressions , with ε_{GE} and ε_{BF} as constants, are valid providing ε_{GE} and ε_{BF} do not vary with the variable plotted in V(G) and V(B). Equations (1) and (2) can be rewritten as :

$$V(E) = \frac{V(G) - (1 - \varepsilon_{BF})V(A)}{\varepsilon_{GE} + \varepsilon_{BF} - 1} \quad (3)$$

$$V(F) = \frac{V(B) - (1 - \varepsilon_{GE})V(A)}{\varepsilon_{GE} + \varepsilon_{BF} - 1} \quad (4)$$

Where $V(A) = V(G) + V(B) = V(E) + V(F)$. An alternative form is given below: [1]

$$V(E) = \frac{\varepsilon_{BF}V(G) - (1 - \varepsilon_{BF})V(B)}{\varepsilon_{GE} + \varepsilon_{BF} - 1} \quad (5)$$

$$V(F) = \frac{\varepsilon_{GE}V(B) - (1 - \varepsilon_{GE})V(G)}{\varepsilon_{GE} + \varepsilon_{BF} - 1} \quad (6)$$

Figure 6 shows the spectra for W+all for $\not{E}_T$(G), $\not{E}_T$(B), $M_T^{e\nu}$(G)($\not{E}_T > 25$), and $M_T^{e\nu}$(B)($\not{E}_T > 25$), where $M_T^{e\nu}$($\not{E}_T > 25$) is the transverse $e\nu$ mass for events with $\not{E}_T > 25GeV$.

4.2 Evaluation of ε_{BF}

Spectra $\not{E}_T$(E) and $M_T^{e\nu}$(E) are plotted for different values of $(1 - \varepsilon_{BF})$. If the value choosen is too large, $\not{E}_T$(E) and $M_T^{e\nu}$(E) have negative values. If $(1 - \varepsilon_{BF})$ is too small the plots of $\not{E}_T$(E) and $M_T^{e\nu}$(E) show signals from the W sitting upon a background. Peaks are seen at about 5 GeV in $\not{E}_T$(E) and at about 25GeV in $M_T^{e\nu}$(E) see Fig. 7. These peaks could be from real electrons (other than $W \to e\nu$), or could be from fake electrons. Figure 8 shows the size of these two low energy peaks as a function of $(1 - \varepsilon_{BF})$. A value of $(1 - \varepsilon_{BF}) = 0.20$ removes almost all of the low energy data. Figure 8 also shows the size of the peaks for data with a cut on $\frac{dE}{dX}$ $(0.6 < \frac{dE}{dX} < 1.3MIP)$. The reduction in the possible signal is a factor of 7 compared to 1.2 for the real W signal (this is from the efficiency of the $\frac{dE}{dX}$ cut used). The major part of the low energy peaks are from fakes and not from real electrons. The value of $(1 - \varepsilon_{BF})$ to remove most of the fake peaks but to produce no negative values is:

$$(1 - \varepsilon_{BF}) = 0.19 \pm 0.01$$
$$\varepsilon_{BF} = 0.81 \pm 0.01$$

[1] If PAW is used equations (5) and (6) are the best to use as the errors are then correctly evaluated. V(G) and V(A) have common events and hence PAW gives incorrect errors if equations (3) and (4) are used.

4.3 Evaluation of ε_{GE}

$(1-\varepsilon_{GE})$ can be evaluated by studying $\not{E}_T$(F) and $M_T^{e\nu}$(F) (i.e. spectra for fake electrons) see equation (4). If $(1-\varepsilon_{GE})$ is too large, negative values are seen in the fake spectra at high energy. If $(1-\varepsilon_{GE})$ is too small peaks are seen in the fake spectra corresponding to a W signal. In practice $(1-\varepsilon_{GE})$ is made as large as possible without producing negative values. This gives:

$$\begin{aligned}(1-\varepsilon_{GE}) &= 0.18 \pm 0.02 \\ \varepsilon_{GE} &= 0.82 \pm 0.02\end{aligned}$$

4.4 Results for W+jets

The values of $\varepsilon_{GE} = 0.82 \pm 0.02$ and $\varepsilon_{BF} = 0.81 \pm 0.01$ are used for the analysis of all channels of W+jets. The signal is extracted by forming the electron signal in $M_T^{e\nu}$(E) with $\not{E}_T \ > 25GeV$ and summing the values between 50 and 95 GeV/c^2, see Fig. 9.

Spectra for the electron signal, ($\not{E}_T$(E) and $M_T^{e\nu}$(E)), and for the fake signal, ($\not{E}_T$(F) and $M_T^{e\nu}$(F)), are also produced without the $\not{E}_T > 25$ GeV cut. These signal and fake spectra give information on the background to W+jets. Figure 10 shows the real electron signal, $M_T^{e\nu}$(E), for; W+0, W+1, W+2, and W+3jets. Figure 11 shows the fake spectra, $M_T^{e\nu}$(F), for; W+0, W+1, W+2, and W+3jets.

Table 3 gives the results for the inclusive channel W+all and the exclusive channels W+0, W+1, W+2, and W+3jets. The table also gives the results for the standard method (from Table 2) corrected for the efficiency ε_{GE}. The values from Table 2 are multiplied by $\frac{1}{\varepsilon_{GE}} = 1.22$

The agreement between the standard method and the fitting method is excellent.

Table 3: Results for W+jets using the fitting method.

	$\varepsilon_{GE} = 0.82$ and $\varepsilon_{BF} = 0.81$	$\varepsilon_{GE} = 0.82$ and $\varepsilon_{BF} = 0.82$	1.22*(Standard method)
W+all	11496 ± 128	11517 ± 127	11496 ± 128
W+0jets	9914 ± 118	9928 ± 118	9902 ± 112
W+1jet	1334 ± 44	1339 ± 44	1309 ± 43
W+2jets	215 ± 18	216 ± 18	212 ± 18
W+3jets	32 ± 7	32 ± 7	32 ± 7

4.5 Systematic Errors

For the fitting method it is necessary to allow for:

- errors in ε_{BF}
- errors in ε_{GE}
- inadequacy of the basic treatment.

4.5.1 Uncertainties in ε_{BF}

Table 3 also shows the results for an assumed value of $\varepsilon_{BF} = 0.82$ as well as for 0.81. The change in the results are 0.2%, 0.1%, 0.4%, 0.5% and 1.6% respectively for W+all, W+0, W+1, W+2, and W+3jets. The change of 0.01 in ε_{BF} corresponds to the estimated uncertainty and hence the errors listed above correspond to about 1 σ.

4.5.2 Uncertaities in ε_{GE}

Equation (3) shows the relationship between ε_{GE} and the signal deduced. ε_{GE} only produces a scaling to correct for the inefficiency of the cuts used to define a good electron. From equation 3:

$$\frac{\delta V(E)}{V(E)} = -1.6\delta\varepsilon_{GE} \tag{7}$$

Hence the uncertainty in the W+jets signal is about $\pm 3.2\%$ from the ± 0.02 uncertainty in ε_{GE}. The assessment of the error for ε_{GE} is somewhat subjective and is taken as ± 0.02 at the equivalent to 1σ. This is probably an overestimate. This error scales all channels and does not modify the relative values.

4.5.3 Possible inadequacy of the fitting procedure

ε_{GE} and ε_{BF} are assumed to be independent of:

- the value of $\not{E}_T$ above 25 GeV
- electron, and fake electron, energy above 25 GeV
- ϕ, θ, and η over the detector.

The first two assumptions are justified and were they incorrect it would have shown up in the analysis. The third assumption is less valid and should be investigated. This has not been carried out in the analysis reported here.

4.5.4 Systematic uncertainties for the standard procedure

Since there is no firm basis for the standard procedure it is very difficult to assign a systematic error uncertainty. This analysis has made no assessment of the appropriate value.

4.6 The form of the Background to W+jets

The background to W+jets can be divided into two forms:

- fake electrons from QCD jets or other sources
- real electrons from a source other than $W \rightarrow e\nu$ (for example from $c\bar{c}$ or $b\bar{b}$).

The first of these is separated out by the fitting method. Figure 12 shows the fake spectra, $M_T^{e\nu}$(F)($\not{E}_T > 25$) with $\not{E}_T > 25GeV$. Figure 11 shows the fake spectra, $M_T^{e\nu}$(F), without the $\not{E}_T$ cut and Fig. 13 shows the fake spectra, $\not{E}_T$(F).

The following comments are relevant:

1. The $M_T^{e\nu}$(F)($\not{E}_T > 25$) spectra peak at the W mass, see Fig. 12.
2. The shape of the $M_T^{e\nu}$(F) plot for W+0jets is very different from that for W+1jet and other channels, see Fig. 11. The W+0jet fake spectra are due a single jet faking an electron and hence $M_T^{e\nu}$ is twice the transverse momentum of the fake jet and it cannot peak at zero since there is the requirement that $E_T("electron") > 25GeV$.
3. W+1jet and other channels show a flat $M_T^{e\nu}$(F) plot at low energy, see Fig. 11, which is reasonable since the event really has $\not{E}_T = 0$.

Background from real electrons from other than $W \rightarrow e\nu$ would show up in the signal plots but with $\not{E}_T$ and $M_T^{e\nu}$ different than the W. Most real electrons will have lower $\not{E}_T$ and $M_T^{e\nu}$ than the W. Since this analysis requires that $E_T(electron) > 25GeV$ most potential sources will be unfavoured. Figures 14 and 10 show the $\not{E}_T$(E) and $M_T^{e\nu}$(E) spectra for real electrons for all channels. Any residual signal other than $W \rightarrow e\nu$ is small. This analysis procedure is not the way to search for such a signal. There is no evidence of a background to $W \rightarrow e\nu$ from other real electrons.

5 Z+jets

The same fitting procedure can be applied to Z+jets. Good Z events are required to have both electrons classified as good. Cuts of $\not{E}_T$(electron 1) $> 25GeV$ and $\not{E}_T$(electron 2) $> 20GeV$ are used.

There are three categories for bad:

- electron 1 good and electron 2 bad
- electron 1 bad and electron 2 good
- electron 1 and electron 2 both bad.

With these definitions equations 1 to 6 can be rewritten as:

$$\begin{aligned}
V^Z(G) &= (\varepsilon_{GE})^2 V^Z(E) + (1-\varepsilon_{BF})^2 V^Z(F) \\
&= 0.672 V^Z(E) + 0.036 V^Z(F) && (8) \\
V^Z(B) &= (1-\varepsilon_{GE}^2) V^Z(E) + (1-(1-\varepsilon_{BF})^2) V^Z(F) \\
&= 0.328 V^Z(E) + 0.964 V^Z(F) && (9) \\
V^Z(E) &= \frac{V^Z(G) - (1-\varepsilon_{BF})^2 V^Z(A)}{\varepsilon_{GE}^2 - (1-\varepsilon_{BF})^2} \\
&= \frac{V^Z(G) - 0.036 V^Z(A)}{0.636} && (10) \\
V^Z(F) &= \frac{V^Z(B) - (1-\varepsilon_{GE}^2) V^Z(A)}{\varepsilon_{GE}^2 - (1-\varepsilon_{BF})^2} \\
&= \frac{V^Z(B) - 0.328 V^Z(A)}{0.636} && (11) \\
V^Z(E) &= \frac{(1-(1-\varepsilon_{BF})^2) V^Z(G) - (1-\varepsilon_{BF})^2 V^Z(B)}{\varepsilon_{GE}^2 - (1-\varepsilon_{BF})^2} \\
&= 1.515 V^Z(G) - 0.057 V^Z(B) && (12) \\
V^Z(F) &= \frac{\varepsilon_{GE}^2 V^Z(B) - (1-\varepsilon_{GE}^2) V^Z(G)}{\varepsilon_{GE}^2 - (1-\varepsilon_{BF})^2} \\
&= 1.057 V^Z(B) - 0.515 V^Z(G) && (13)
\end{aligned}$$

The values of ε_{GE} and ε_{BF} deduced from the W+jets analysis should apply also to Z+jets.

The bad electron events have to be corrected to remove jets from the jet list corresponding to the fake electrons to avoid double counting. For the background where both electrons are bad, 2 jets have to be removed and for the events where only one electron is bad, one jet has to be removed.

Figure 15 shows for all Z events the extracted M^{ee}(E) real signal and the M^{ee}(F) fake signal. Figure 16 shows the real signal plots, M^{ee}(E), for Z+0jets, Z+1jet, and Z+2jets. The parameters determined from the W+jets analysis provide a good solution for Z+jets.

Table 4 gives the results for $82 < M^{ee}(\text{E}) < 100 GeV/c^2$ for Z+0jets, Z+1jet, and Z+2jets. Values are given for the number of events: N(G), N(B), N(E), N(F), and for the noise to signal ratio.

6 Conclusions

This paper presents an alternative way of evaluating the background to W+jets and Z+jets. The results are in agreement with the standard method. It has the advantage that it provides new insight into the form of the background.

Table 4: Results for Z+jets

	N(G)	N(B)	N(E)	N(F)	noise/signal in V(G)
Z+all	521 ± 23	820 ± 29	743 ± 35	598 ± 33	4.3%
Z+0jets	428 ± 21	618 ± 25	613 ± 31	433 ± 28	3.8%
Z+1jet	77 ± 9	143 ± 12	109 ± 13	111 ± 13	5.5%
Z+2jets	13 ± 4	35 ± 6	18 ± 6	30 ± 6	9.2%

It is based upon a procedure that has wider applicability and since it has a well formulated basis it is possible to evaluate the statistical and systematic uncertainties.

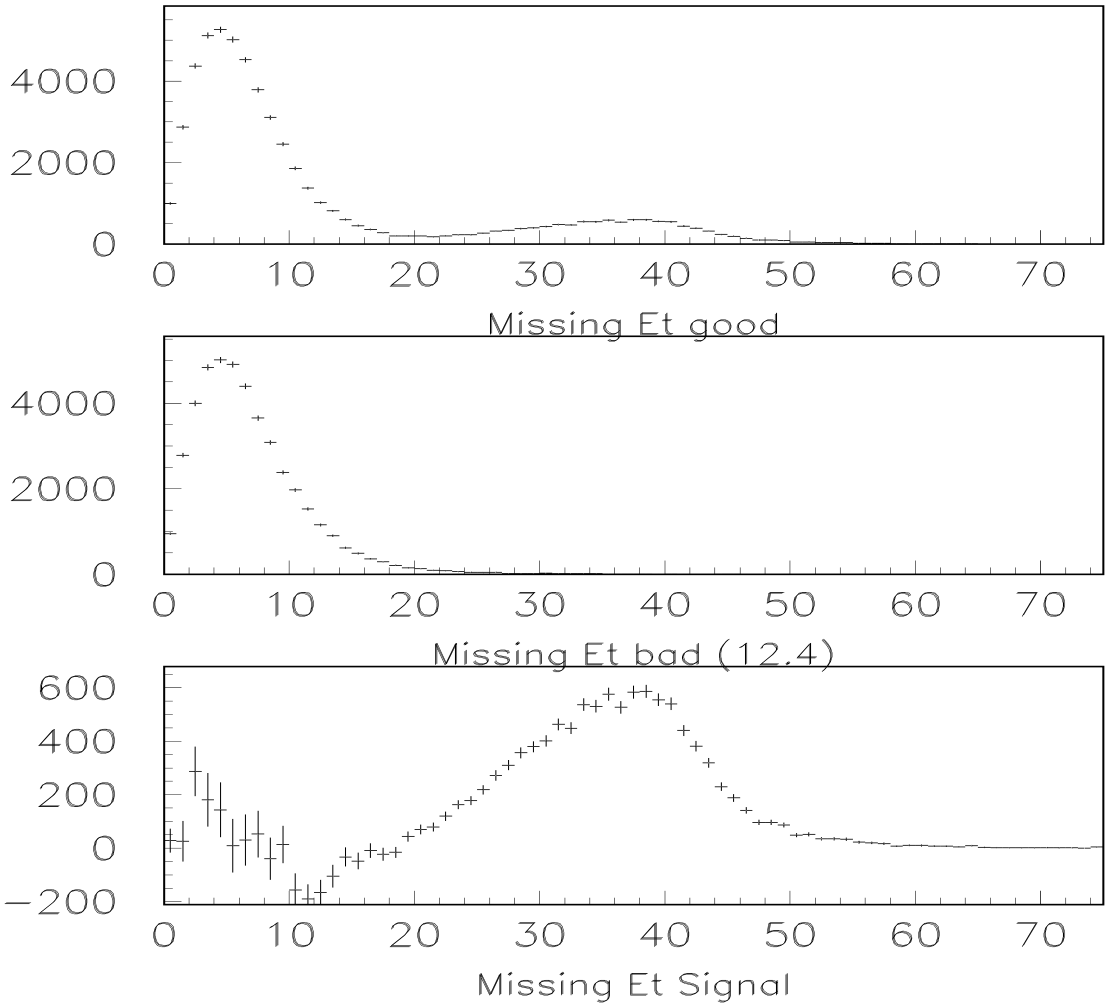

Figure 1: Normalisation of background for standard method. W+all events.

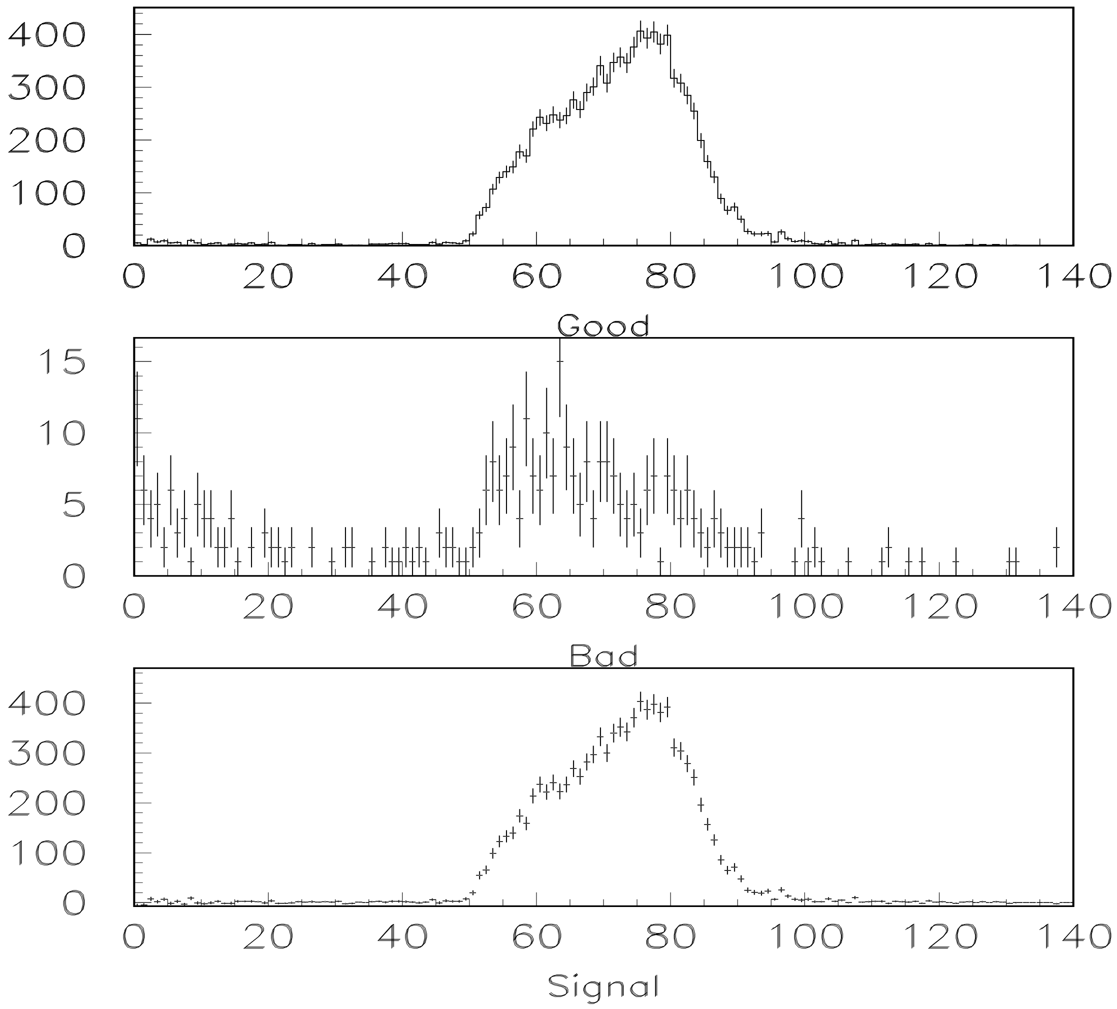

Figure 2: $M_T^{e\nu}$(G)($\not{E}_T > 25$), $M_T^{e\nu}$(B)($\not{E}_T > 25$), and $M_T^{e\nu}$(S)($\not{E}_T > 25$) for W+all events.

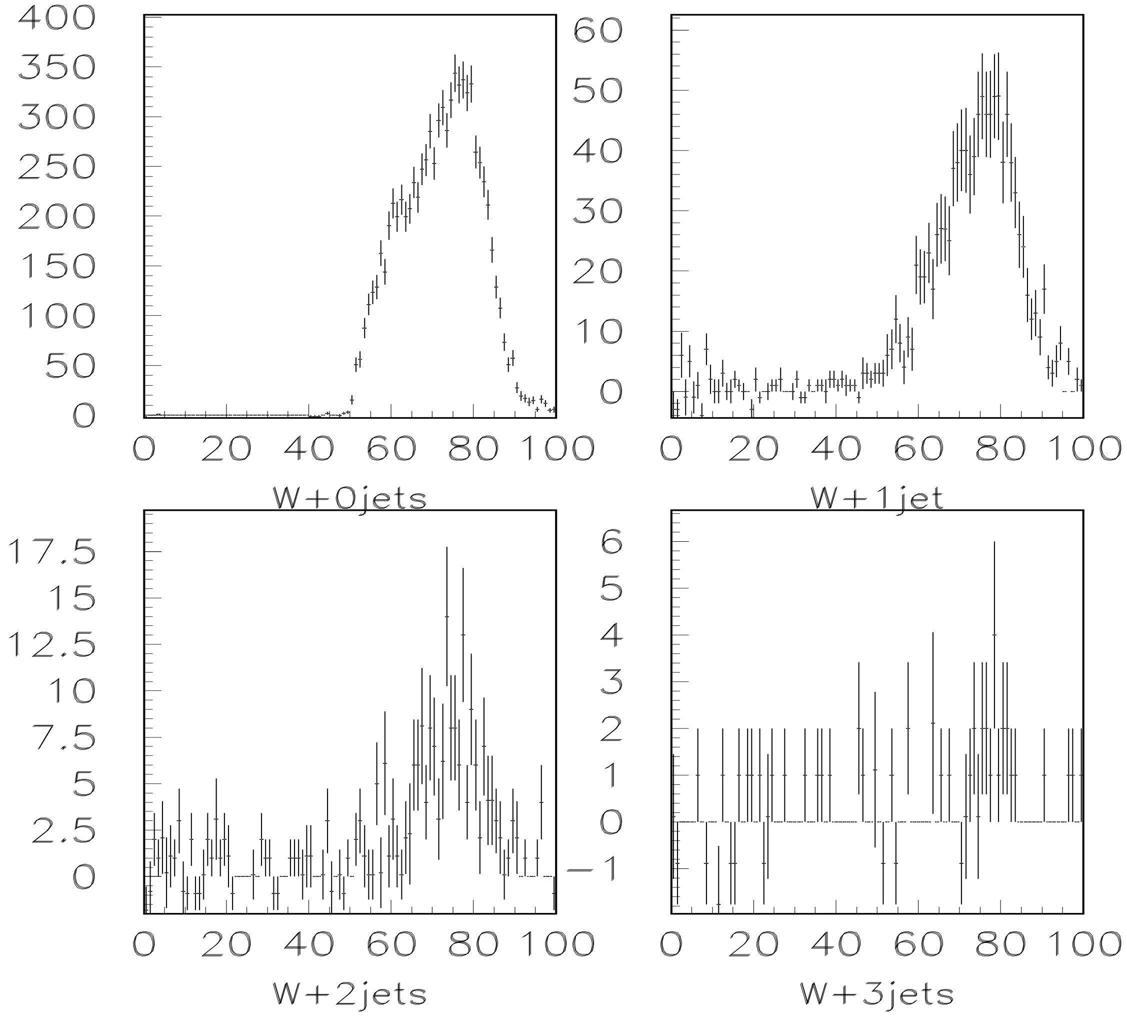

Figure 3: $M_T^{e\nu}$(S)($\not{E}_T > 25$) for W+0jets, W+1jet, W+2jets, and W+3jets.

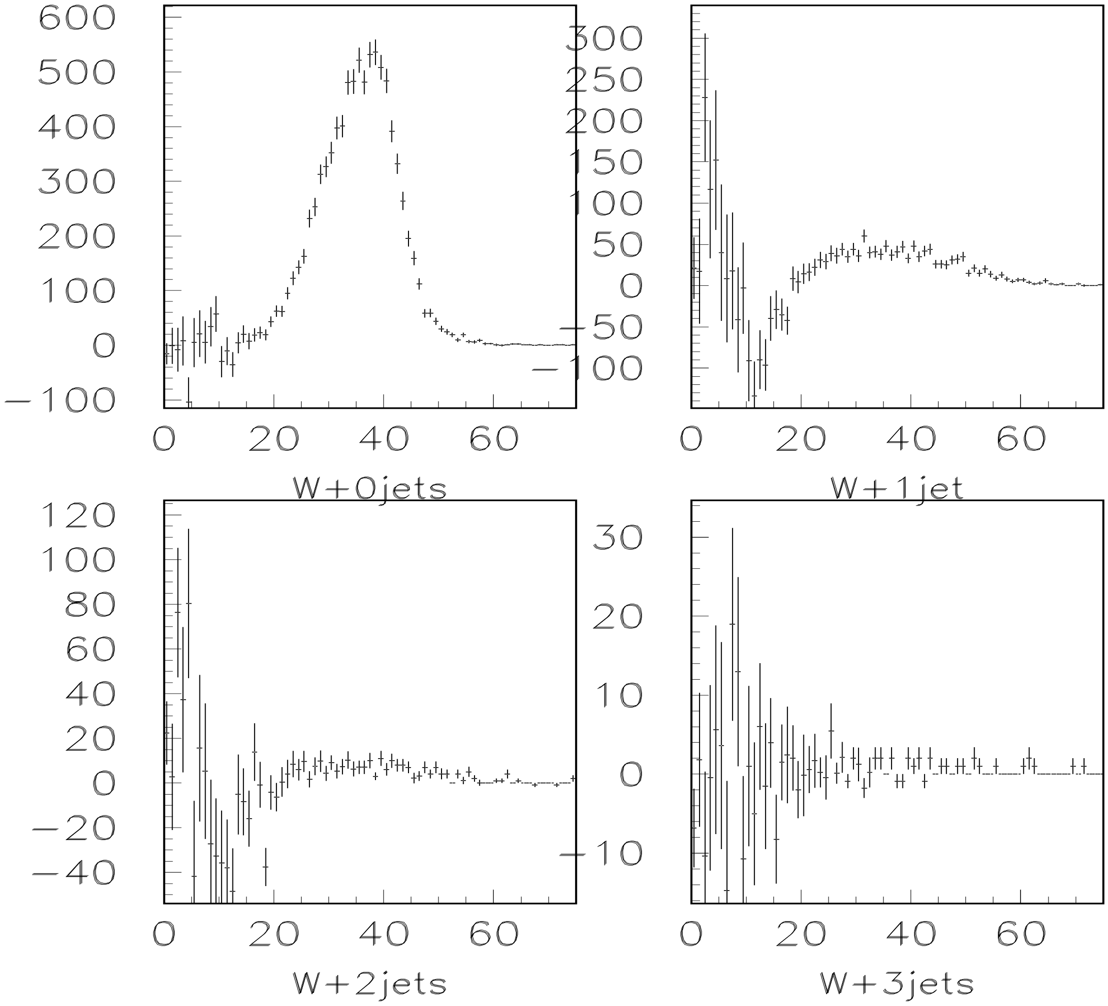

Figure 4: $\not\!\!E_T$(S) for W+0jets, W+1jet, W+2jets, and W+3jets.

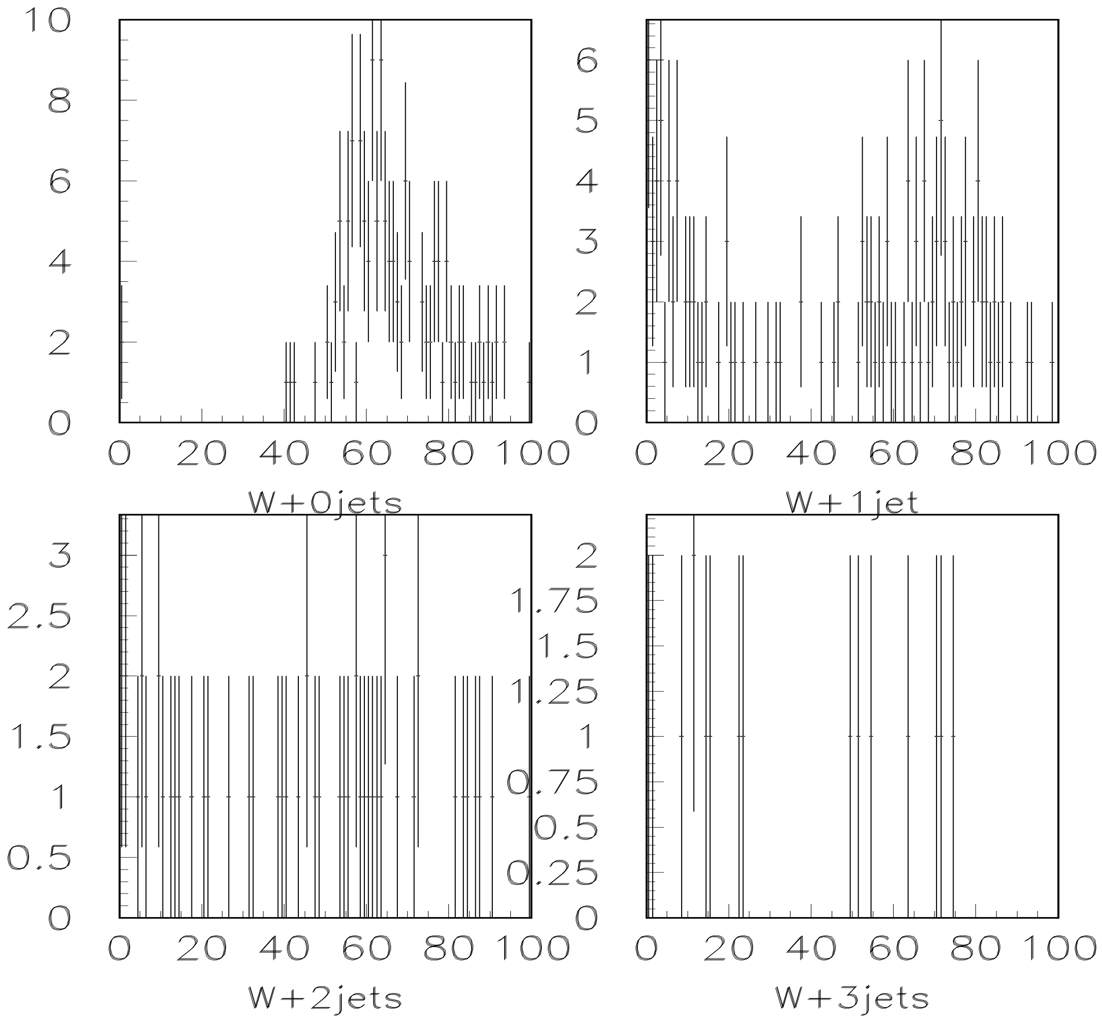

Figure 5: $M_T^{e\nu}$(B)($\not\!\!E_T > 25$) for W+0jets, W+1jet, W+2jets, and W+3jets.

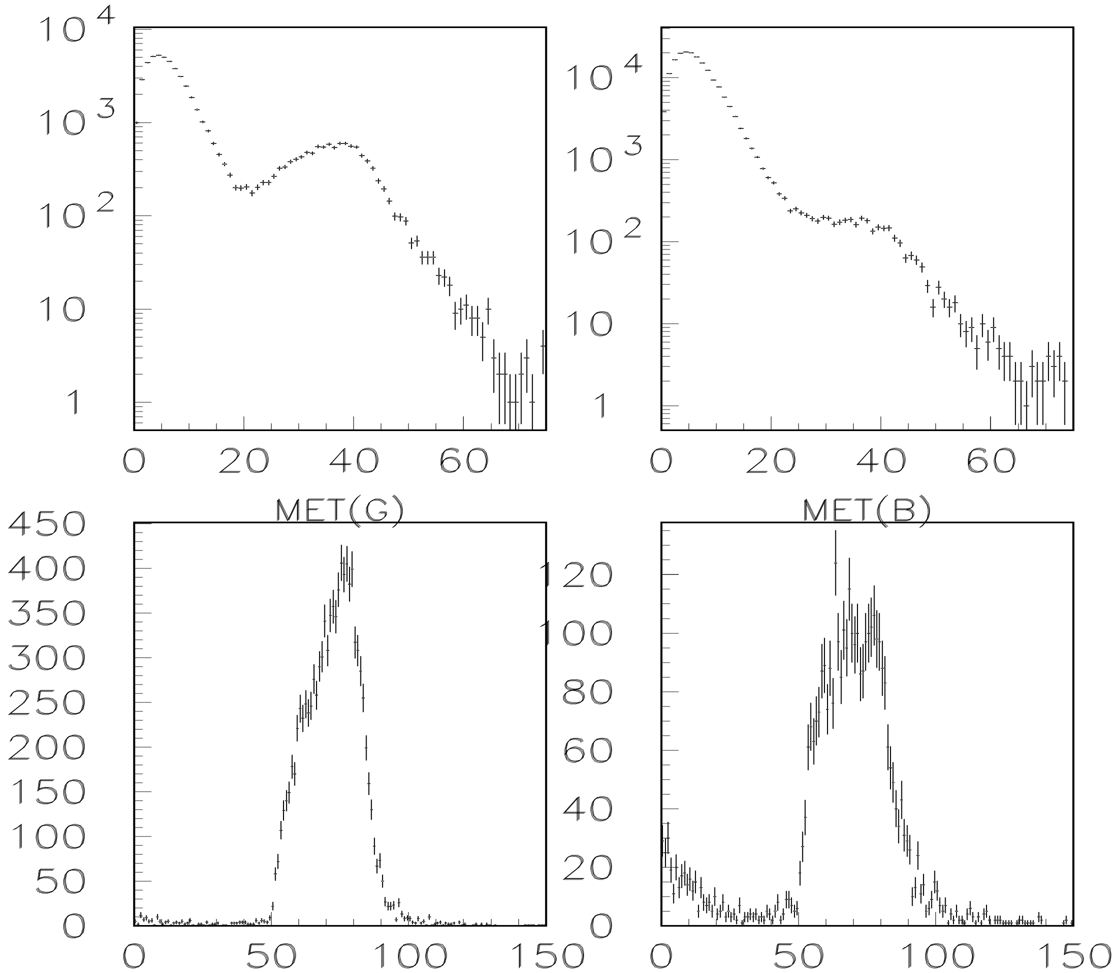

Figure 6: Input spectra used for fitting method for W+all events. The top spectra are $\not\!\!E_T$(G) and $\not\!\!E_T$(B) and the bottom two are $M_T^{e\nu}$(G)($\not\!\!E_T > 25$) and $M_T^{e\nu}$(B)($\not\!\!E_T > 25$)

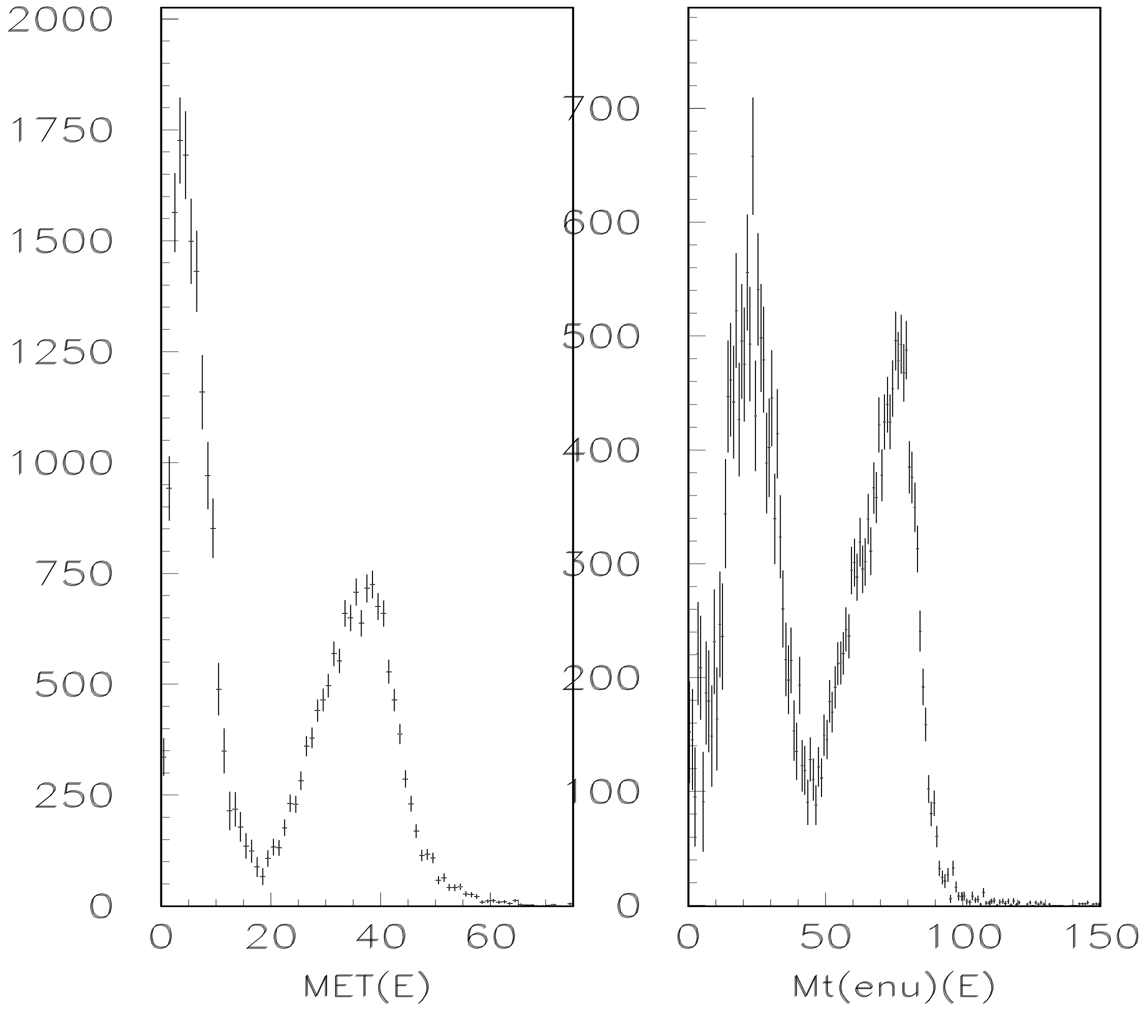

Figure 7: The signals $\not{E}_T$(E) and $M_T^{e\nu}$(E) using equation (5) with $\varepsilon_{GE} = 0.82$ and $\varepsilon_{BF} = 0.84$ for W+all events.

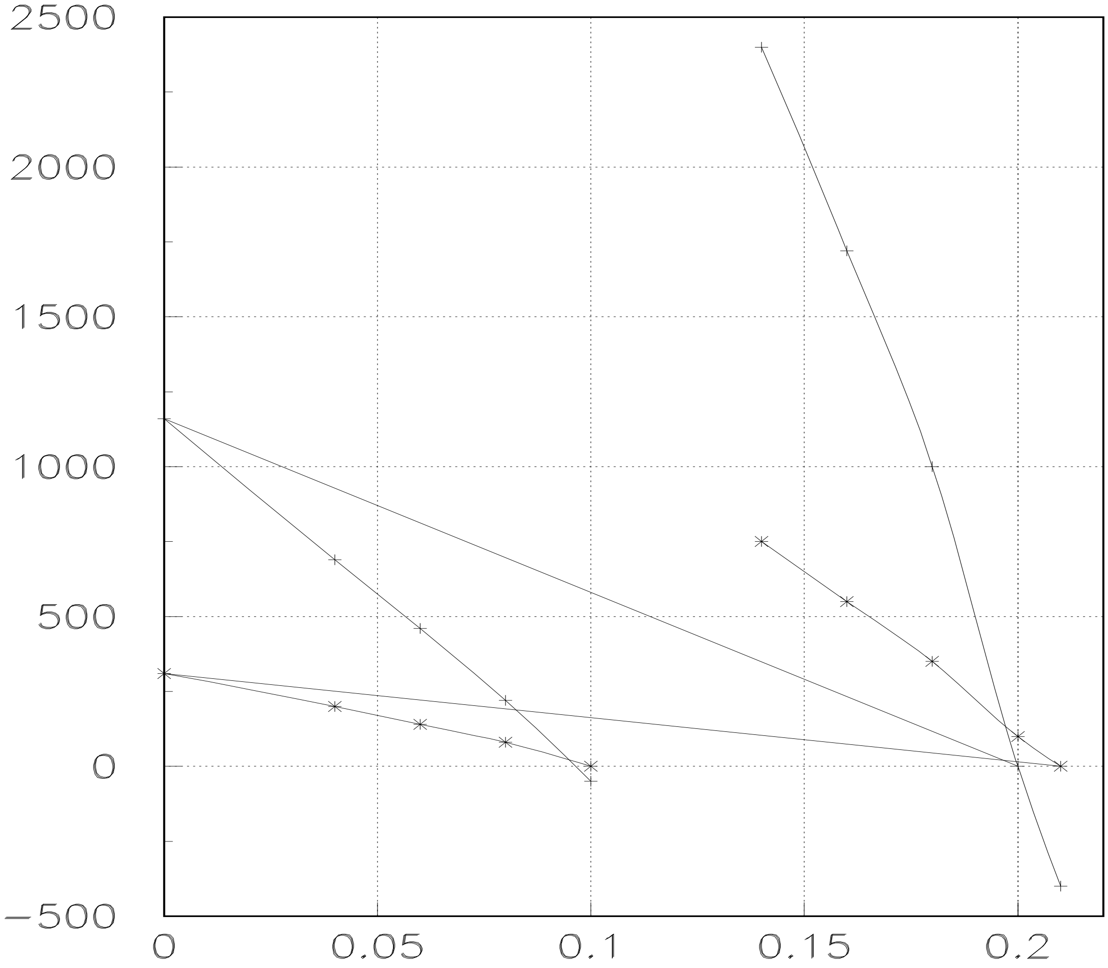

Figure 8: Height of low energy peaks against (1-ε_{BF}). The two lines to the right are for data without a $\frac{dE}{dX}$ cut. The two lines to the left are for data with a $\frac{dE}{dX}$ cut. The lines marked with a "$*$" are for the $M_T^{e\nu}(25)$ peak and those marked with a "$+$" are for the $\not{E}_T(5)$ peak. The plots with a $\frac{dE}{dX}$ cut give a zero peak height at (1-ε_{BF}) of 0.1 compared to 0.2 with no $\frac{dE}{dX}$ cut. This change in ε_{BF} is because the $\frac{dE}{dX}$ cut decreases the fake electron contribution. The lines for the plots with the $\frac{dE}{dX}$ cut are scaled to give zero peak height at the same value of (1-ε_{BF}) - see unlabeled lines. These scaled lines are a factor of 7 below those with no $\frac{dE}{dX}$ cut.

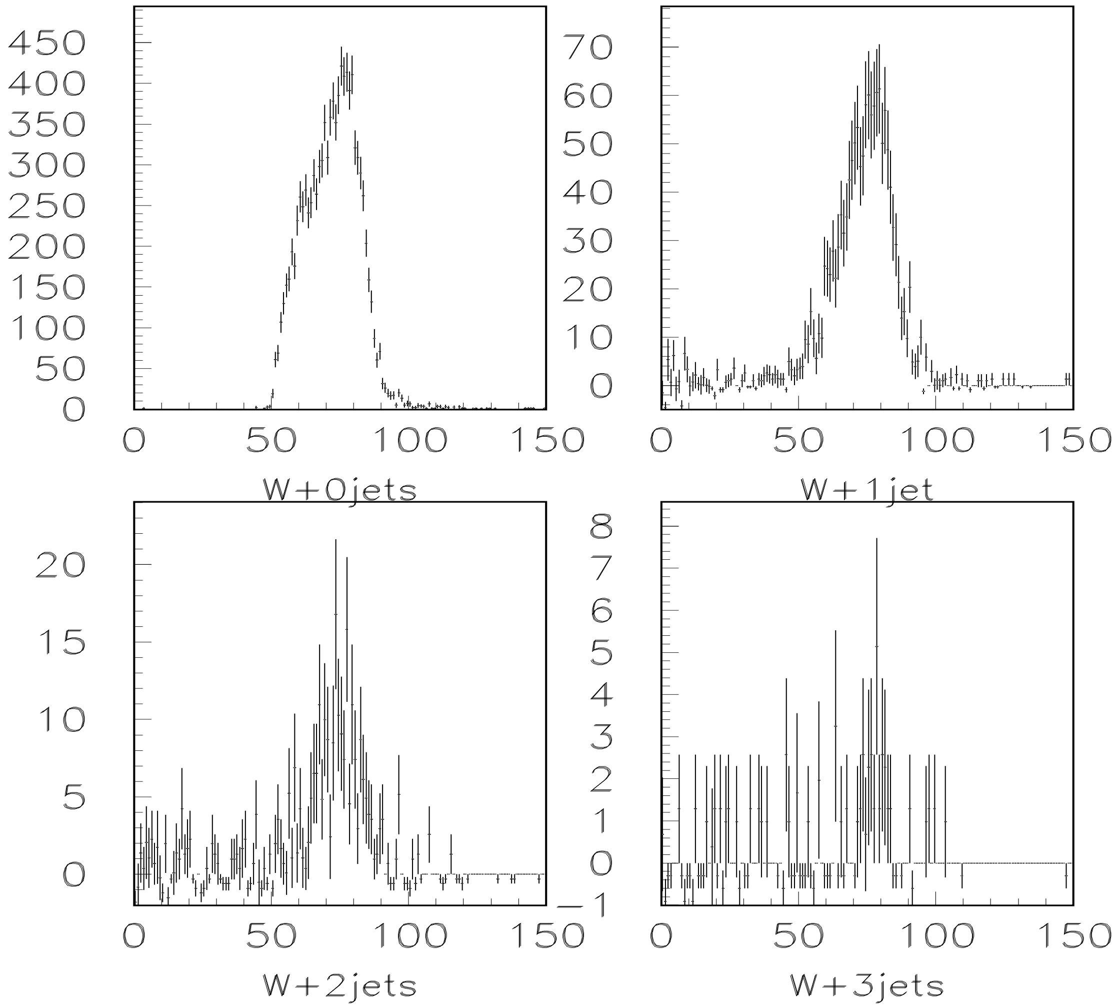

Figure 9: $M_T^{e\nu}$(E)($\not{E}_T > 25$) for W+0jets, W+1jet, W+2jets, and W+3jets. The signal is taken by summing values between 50 and 95 GeV/c^2.

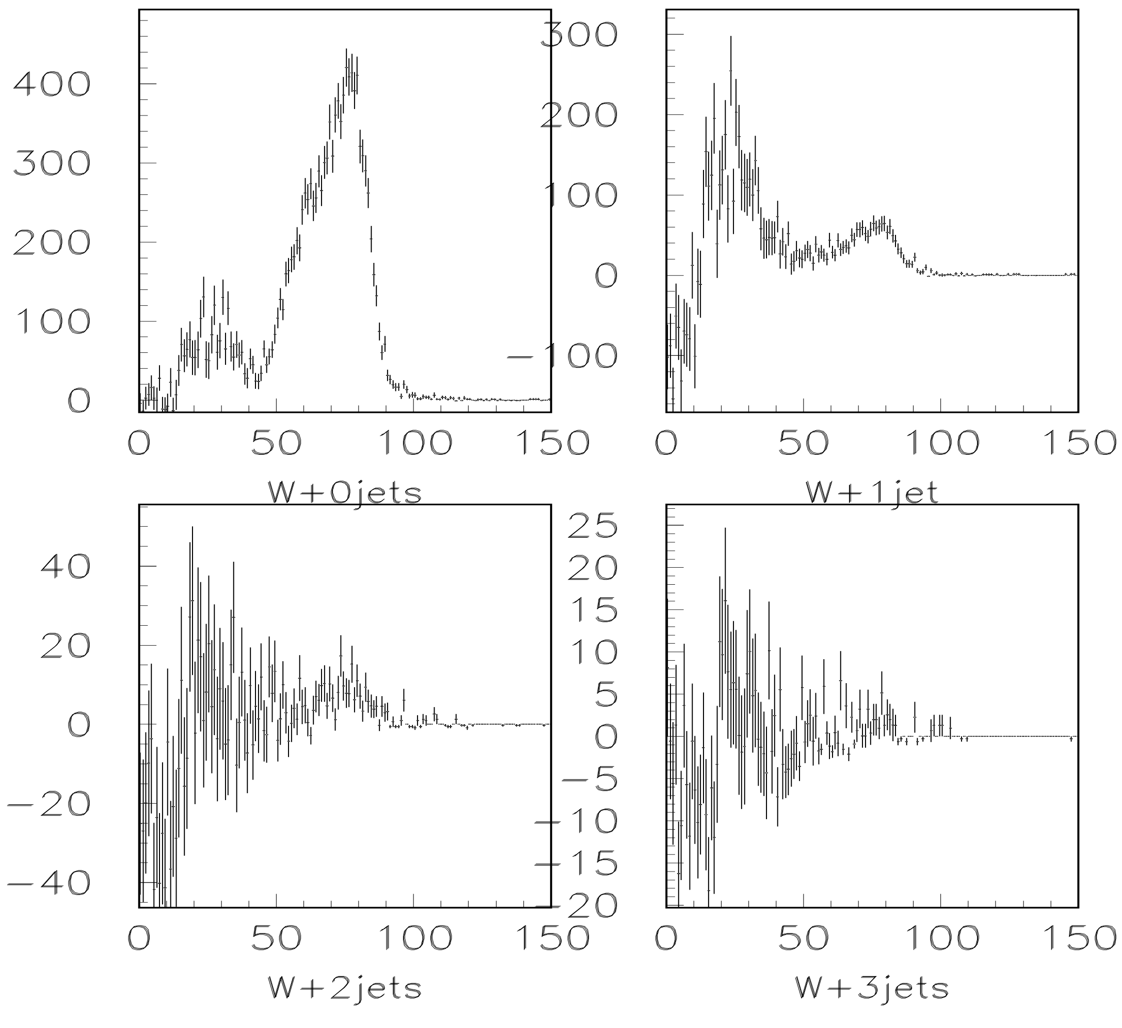

Figure 10: Spectra $M_T^{e\nu}$(E), without $\not{E}_T >$ 25 cut, for W+0jets, W+1jet, W+2jets, and W+3jets.

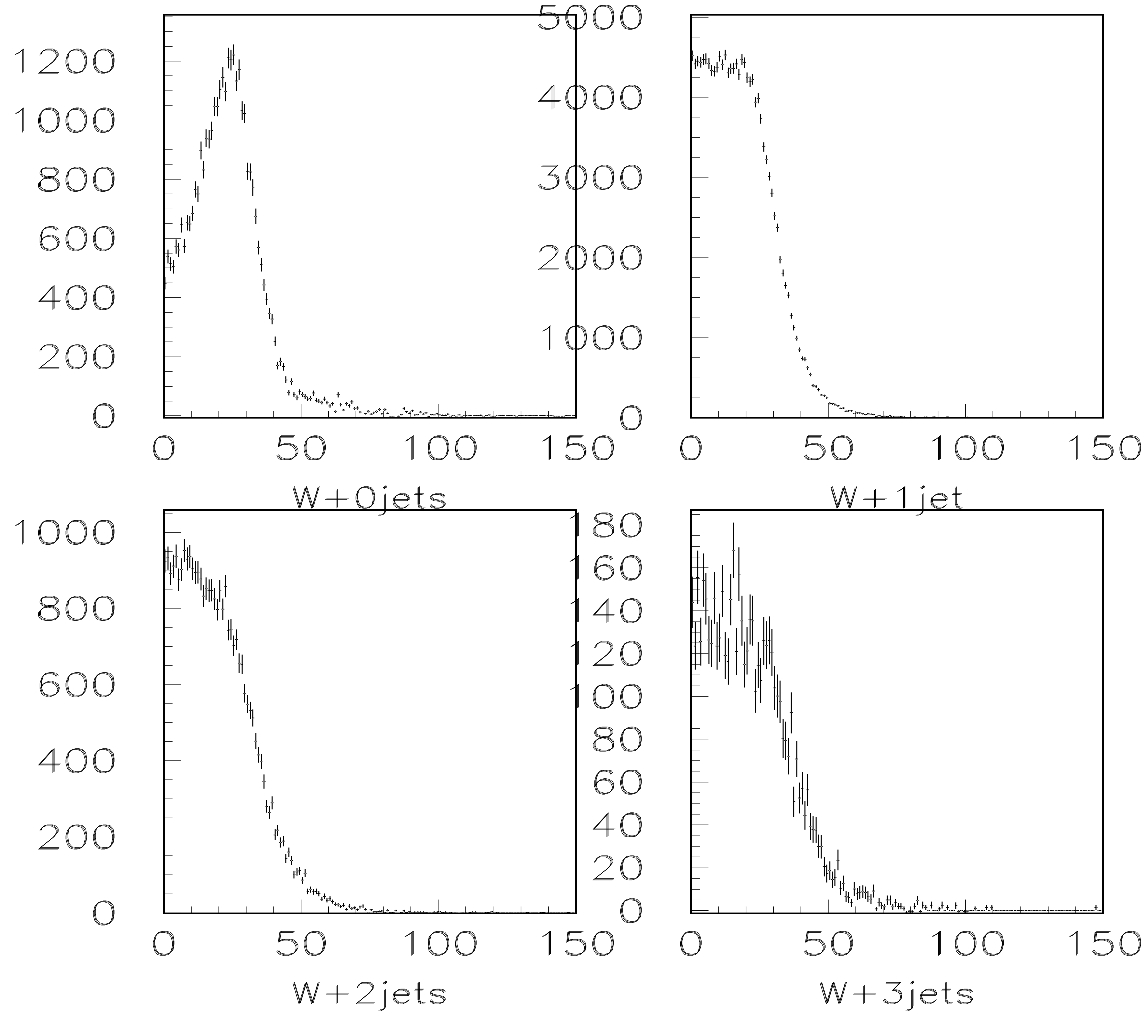

Figure 11: Fake electron spectra $M_T^{e\nu}(\mathrm{F})$, without $\not{E}_T > 25$ cut, for W+0jets, W+1jet, W+2jets, and W+3jets.

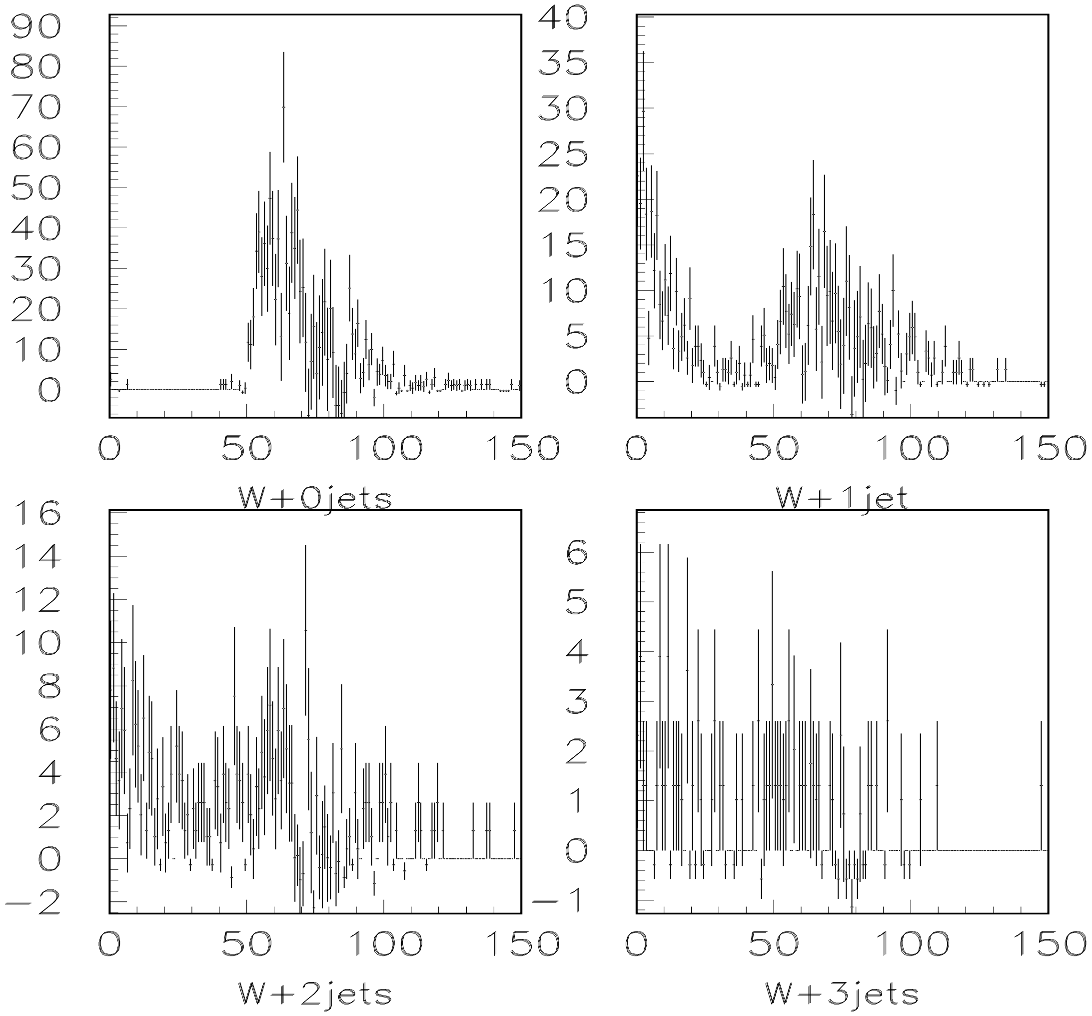

Figure 12: Fake electron spectra $M_T^{e\nu}(\mathrm{F})(\not{E}_T > 25)$ for W+0jets, W+1jet, W+2jets, and W+3jets.

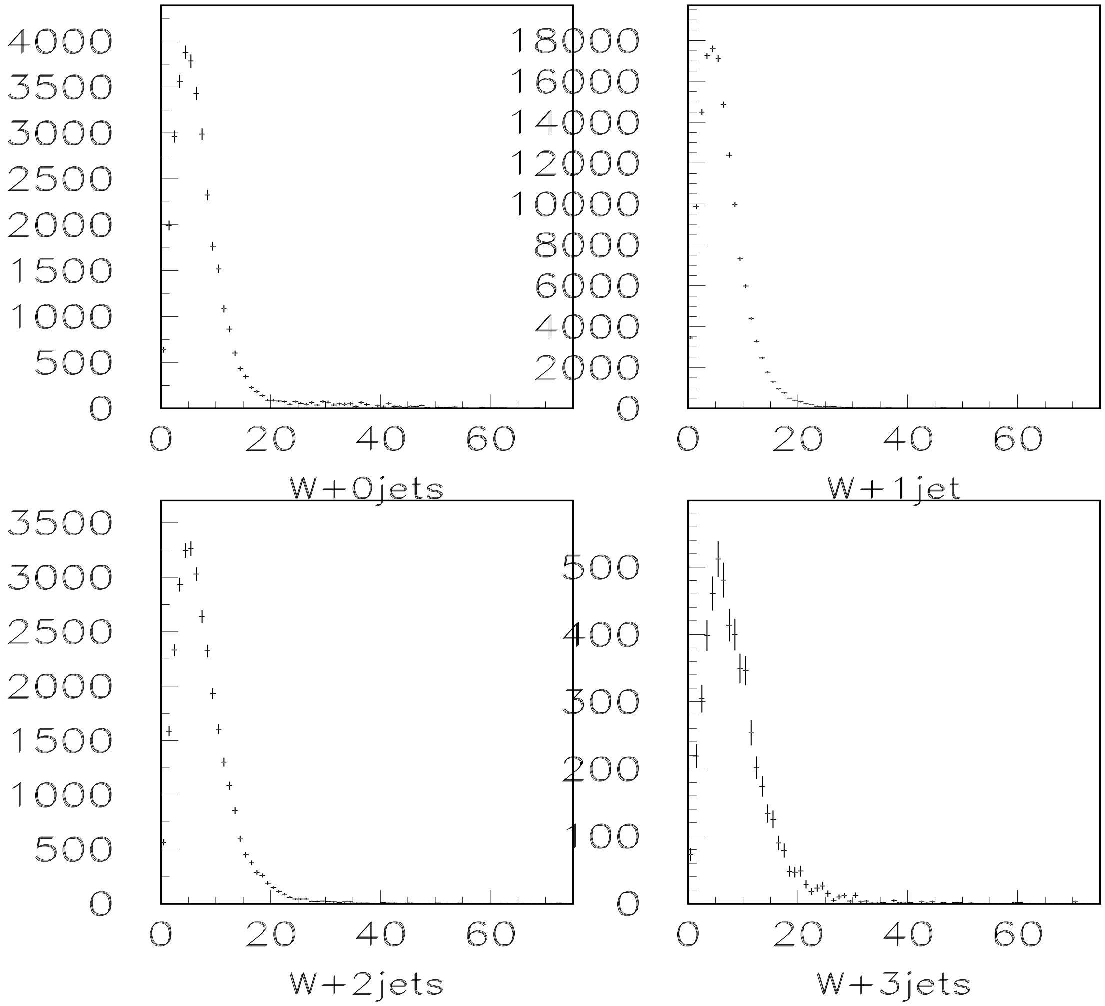

Figure 13: Fake electron spectra $\not{E}_T$(F) for W+0jets, W+1jet, W+2jets, and W+3jets.

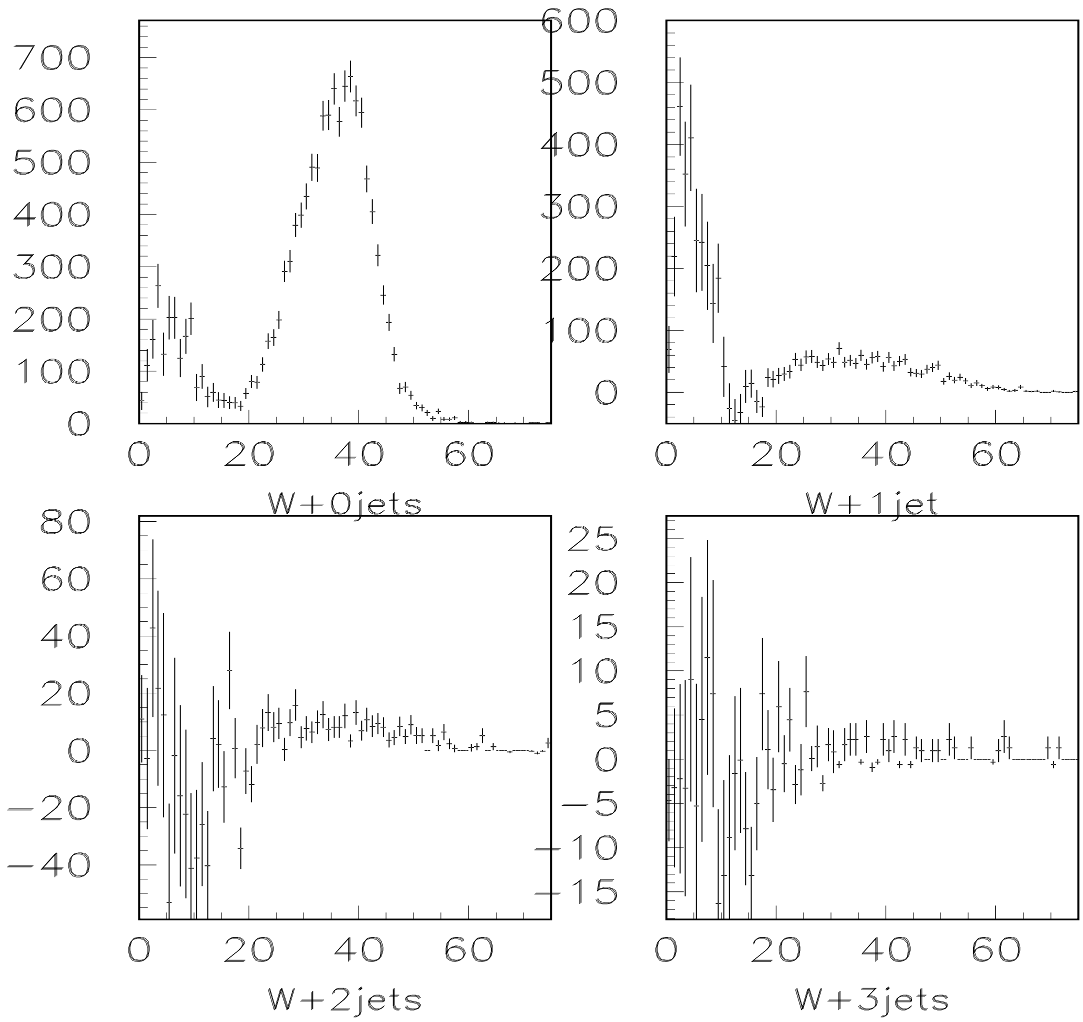

Figure 14: Spectra $\not{E}_T$(E) for W+0jets, W+1jet, W+2jets, and W+3jets.

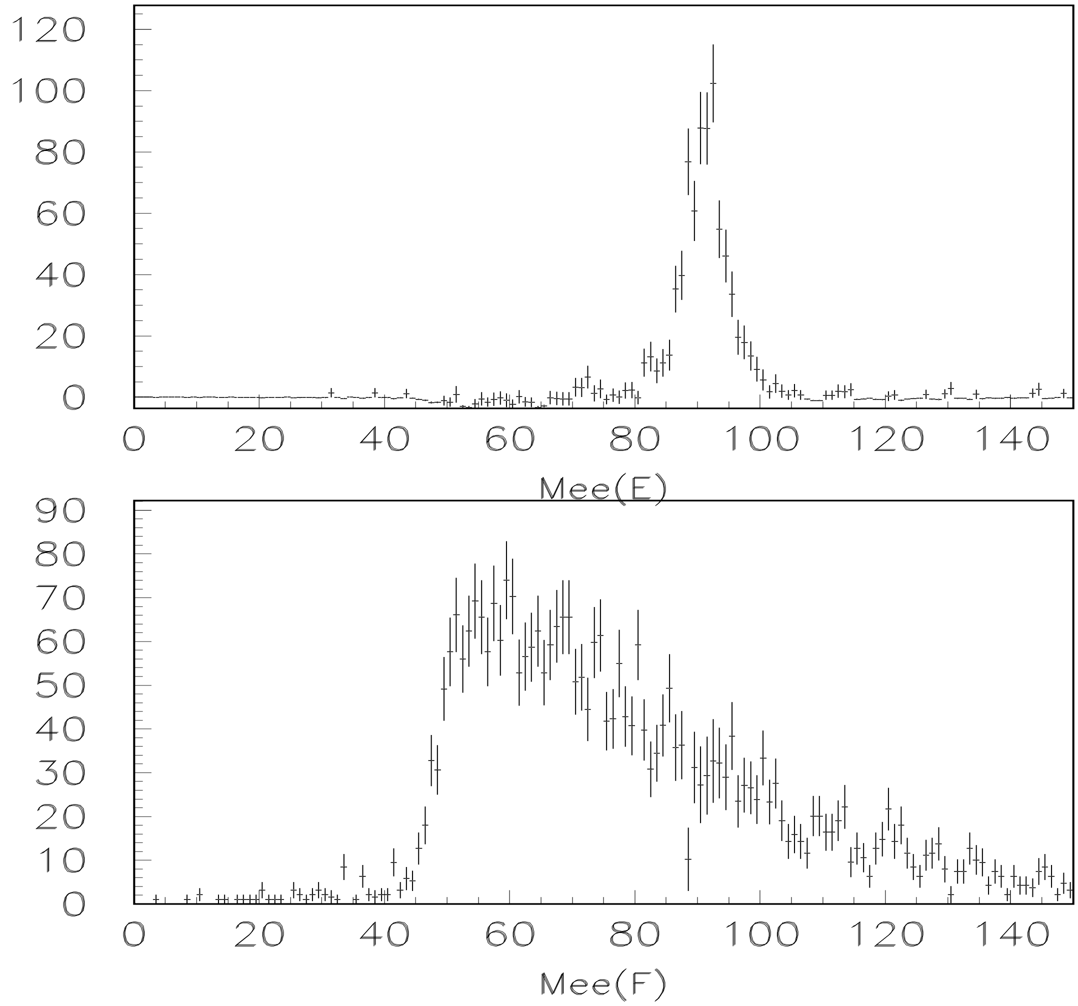

Figure 15: The spectra M^{ee}(E) and M^{ee}(F) for Z+all events.

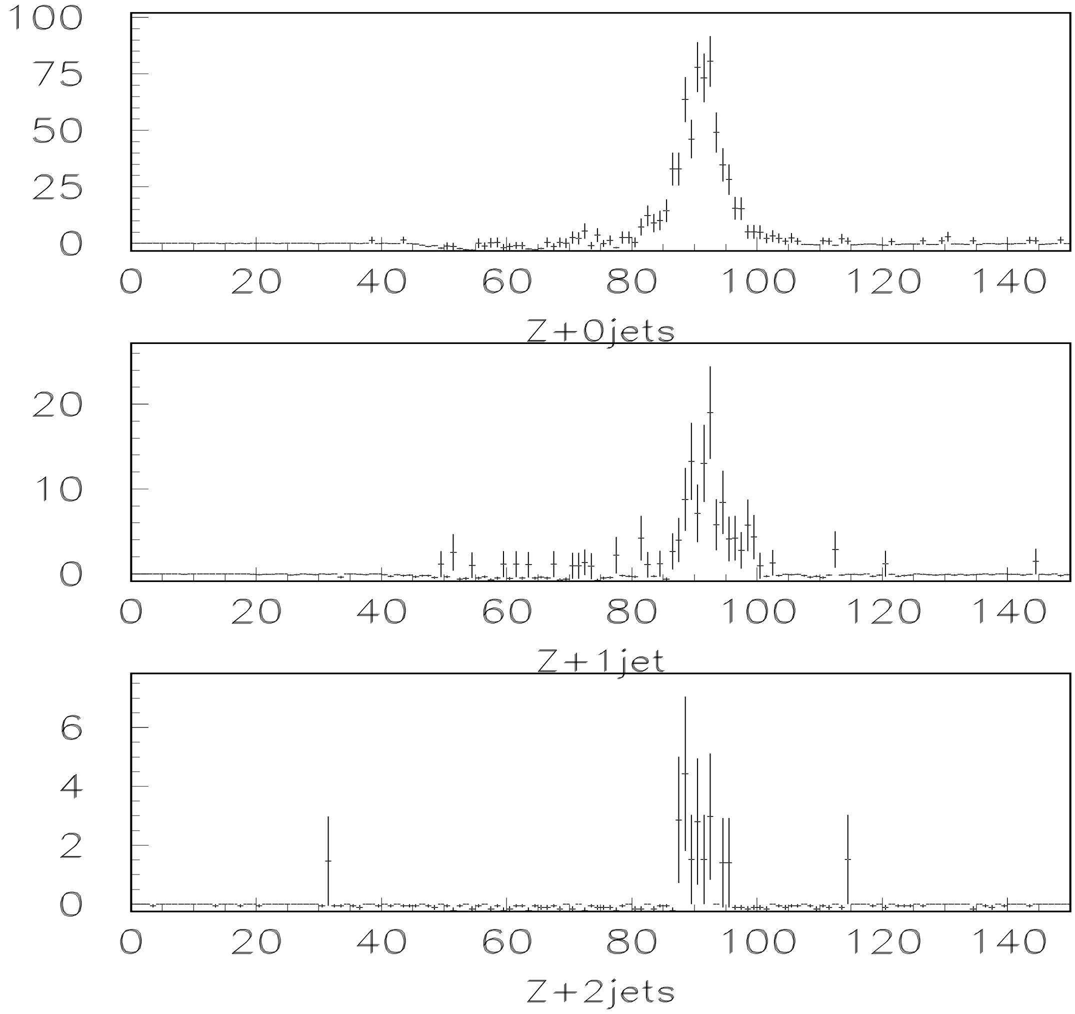

Figure 16: The spectra M^{ee}(E) extracted using equation (12) for Z+0jets, Z+1jet, and Z+2jets. The signal is evaluated by summing the values between 82 and 100 GeV/c^2